Interference of ALOX5 alleviates inflammation and fibrosis in high glucose-induced renal mesangial cells

XIAOTAO CHEN[1], HONGWU XIE[2], YUN LIU[1], QIUJUAN OU[3] and SHUAIJIE DENG[4]

[1]Department of Endocrinology, Affiliated Hospital of Xiangnan University, Chenzhou, Hunan 423000;
[2]Department of Endocrinology, The Fourth People's Hospital of Chenzhou, Chenzhou, Hunan 423001;
[3]Department of Nephrology, Affiliated Hospital of Xiangnan University, Chenzhou, Hunan 423000;
[4]Century College, Beijing University of Posts and Telecommunications, Beijing 102101, P.R. China

Received August 22, 2021; Accepted September 6, 2022

DOI: 10.3892/etm.2022.11733

Abstract. Diabetic nephropathy (DN) is the leading cause of end-stage renal disease (ESRD), seriously threatening the health of individuals. The 5-lipoxygenase (ALOX5) gene has been reported to be associated with diabetes, but whether it is involved in DN remains unclear. The present study aimed to explore the role of ALOX5 in DN and to clarify the potential mechanism. Mouse renal mesangial cells (SV40 MES-13) were treated with high glucose (HG) to mimic a DN model *in vitro*. The expression level of ALOX5 was assessed using reverse transcription-quantitative PCR and western blotting. Cell Counting Kit-8 and flow cytometric assays were performed to determine cell proliferation, the cell cycle and apoptosis. Immunofluorescence was carried out to detect the expression of Ki67 and proliferating cell nuclear antigen (PCNA). The inflammatory cytokines were assessed using ELISA. The expression of fibrosis- and NF-κB-related proteins was determined using western blotting. The results revealed that ALOX5 was significantly upregulated in HG-induced SV40 MES-13 cells. Interference of ALOX5 greatly hindered HG-induced cell viability loss, as well as increasing the expression of Ki67 and PCNA. In addition, HG induced cell cycle arrest in the G1 phase and cell apoptosis, which were then partly abolished by interference of ALOX5. Moreover, the elevated production of inflammatory cytokines and upregulated fibrosis-related proteins induced by HG were weakened by interference of ALOX5. Eventually, interference of ALOX5 was found to reduce the activity of NF-κB signaling in HG-induced SV40 MES-13 cells. Collectively, interference of ALOX5 serves as a protective role in HG-induced kidney cell injury, providing a potential therapeutic strategy of DN treatment.

Correspondence to: Dr Xiaotao Chen, Department of Endocrinology, Affiliated Hospital of Xiangnan University, 25 Renmin West Road, Beihu, Chenzhou, Hunan 423000, P.R. China
E-mail: chenxtxt2012@163.com

Key words: 5-lipoxygenase, renal mesangial cells, high glucose, inflammation

Introduction

Diabetic nephropathy (DN) is a serious complication of diabetes mellitus (DM) clinically characterized as increased urinary albumin excretions, reduced glomerular filtration rate and progressive deteriorations in renal function (1). It is reported that approximately 20-40% of patients with diabetes develop DN in their disease course (2,3). DN is the leading cause of chronic kidney disease (CKD) and end-stage renal disease (ESRD), and is acknowledged as an independent risk factor for cardiovascular diseases, seriously threatening human health (4,5). Currently, strict glycemic, blood pressure, and lipid control are the main managements of DN (1); however, ~40% of diabetic patients progress to ERSD, eventually requiring dialysis, which imposes heavy health care costs (6). Given the increased prevalence of the DN, seeking novel biomarkers for the early detection of DN and elucidating the pathogenesis of DN are essential in order to provide appropriate treatments to prevent this disease.

The 5-lipoxygenase gene (ALOX5), a member of the ALOX family responsible for the oxidative metabolism of polyunsaturated fatty acids, is involved in arachidonate metabolism, a metabolic pathway in which cysteinyl leukotrienes are biosynthetically initiated (7,8). ALOX5 has been reported to be closely associated with multiple physiological and pathological processes, such as inflammation, oxidative stress, and cell differentiation, thus influencing various diseases, including cancers, myocardial infarction, and bone diseases (9-11). Interestingly, ALOX5 was generally reported to be aberrantly upregulated in patients suffering from different diseases, such as esophageal adenocarcinoma and gastric cancer (12,13). Notably, ALOX5 was also reported to be aberrantly upregulated in type 1 diabetes (T1D) and type 2 diabetes (T2D). Increased expression of ALOX5 was linked to the tissue inflammation in diabetes, and the inhibitor of ALOX5 was suggested as a candidate for DM (14-16). In addition, ALOX5 appears to be involved in the progression of diabetic retinal disease, emphasizing the importance of ALOX5 in DM-related diseases (17). In addition, ALOX5-deficient mice with diabetic retinopathy exhibited less leukostasis, superoxide production, and nuclear factor (NF)-κB expression, suggesting that the inflammation in diabetic retinopathy

was ALOX5-dependent (18). Moreover, ALOX5 products have been demonstrated to be involved in renal tubulointerstitial injury, indirectly indicating that ALOX5 is associated with renal tissue injury (19). Furthermore, a previous study demonstrated that although ALOX5 is usually located in leukocytes, dendritic cells, macrophages and neutrophils, it can also be found in areas of the kidney, including the cortex, outer medulla, and inner medulla (20). Collectively, ALOX5 appears to participate into multiple processes of DM-related diseases and renal diseases, as DN is one of the complications of DM, it is hypothesized that ALOX5 may be involved in the progression of DN.

Therefore, the present study aimed to investigate the role of ALOX5 in the progression of DN, and to explore the underlying mechanism of action, addressing the therapeutic potential of ALOX5 in DN. To better carry the exploration, an *in vitro* cell model of DN was first constructed. HG-induced SV40 MES-13 has been widely recognized as an *in vitro* cell model of DN, and has been widely applied in numerous studies (21-24). Accordingly, SV40 MES-13 cells were treated with HG to simulate DN *in vitro* in the present study.

Materials and methods

Cell culture and treatment. Mouse renal mesangial cells (SV40 MES-13) were obtained from American Type Culture Collection and cultured in Dulbecco's modified Eagle's medium (DMEM; Thermo Fisher Scientific, Inc.) supplemented with 10% fetal bovine serum (FBS; Gibco; Thermo Fisher Scientific, Inc.) and 1% streptomycin/penicillin (HyClone; Cytiva) in a 5% CO_2 incubator under 37˚C. Cells were classified into normal glucose (NG; 5.6 mM glucose) and high glucose (HG; 30 mM) groups according to the treatment of various concentrations of glucose for 24 h.

Cell transfection. siRNAs against ALOX5 (si-ALOX5-1, 5'-GCCGGACUGAUGUACCUGUUUTT-3'; si-ALOX5-2, 5'-CCUGUUCAUCAACCGCUUCAUTT-3') and siRNA negative control (si-control, 5'-UUCUCCGAACGUGUCACG UTT-3') were obtained from Shanghai GenePharma Co., Ltd. SV40 MES-13 cells were transfected with si-control (50 nM) or si-ALOX5 (50 nM) using Lipofectamine® 3000 (Invitrogen; Thermo Fisher Scientific, Inc.) at 37˚C. At 48 h post transfection, the transfected cells were harvested for the further experiments.

Cell viability assay. Transfected or non-transfected cells were seeded into 96-well plates ($3x10^3$ cells/well) and then incubated with different doses of glucose. After 24 and 48 h of incubation, 10 μl Cell Counting Kit-8 (CCK-8; Dojindo Molecular Technologies, Inc.) solution was added to each well for another incubation at 37˚C for 1 h in an incubator with 5% CO_2. Finally, the OD value of each group was determined at an absorbance of 450 nm using a microplate reader (Bio-Rad Laboratories, Inc.).

Immunofluorescence. SV40 MES-13 cells were seeded into 6-well plates ($5x10^4$ cells/well) and cultured for 24 h. Then, cells were washed with PBS and fixed with 4% paraformaldehyde for 30 min at room temperature and permeabilized using 0.5% Triton X-100. Subsequently, the cells were blocked in 2.5% bovine serum albumin (BSA) at room temperature for 1 h and incubated with anti-Ki67 (1:500; cat. no. orb389335; Biorbyt Ltd.) or anti- proliferating cell nuclear antigen (PCNA; 1:50; cat. no. orb48485; Biorbyt Ltd.) antibodies at 4˚C overnight. The following day, the cells were incubated with the Alexa Fluor 488-flagged goat anti-rabbit secondary antibody (1:500; cat. no. A0423; Beyotime Institute of Biotechnology). Subsequently, the cells were incubated with DAPI for 3 min, and the fluorescence signals were captured using a DMRA2 fluorescence microscope (Leica Microsystems GmbH).

Flow cytometric analysis. Cell cycle and cell apoptosis were evaluated using a flow cytometer. Briefly, SV40 MES-13 cells were harvested and washed using ice-cold PBS twice. For the cell cycle assay, cells were fixed with 70% ice-cold ethanol overnight. The cells were then incubated with 50 μg/ml RNase at 37˚C for 30 min, followed by staining with 50 μg/ml propidium iodide (PI) at 4˚C for 30 min in the dark. For cell apoptosis assay, cells were resuspended with 500 μl binding buffer, followed by staining with 5 μl Annexin V-FITC and 5 μl PI at room temperature for 15 min in the dark. Finally, the flow cytometric analysis was performed by a FACScan (Beckman Coulter, Inc.) and the data were analyzed using FlowJo software version 10.6.2 (Tree Star, Inc.).

Enzyme-linked immunosorbent assay (ELISA). The concentrations of inflammatory cytokines in the culture medium, including TNF-α, IL-6 and IL-1β, were detected using their corresponding ELISA kits: Mouse TNF-α ELISA kit (cat. no. orb565170), mouse IL-6 ELISA kit (cat. no. orb565132) or mouse IL-8 ELISA kit (cat. no. orb566249) from Biorbyt Ltd., according to the manufacturer's instructions.

Reverse transcription-quantitative PCR (RT-qPCR). The total RNA was extracted from cells using TRIzol reagent (Invitrogen; Thermo Fisher Scientific, Inc.) according to the manufacturer's instructions. The purity of RNA was measured using NanoDrop 2000 spectrophotometer (Thermo Fisher Scientific, Inc.). First-strand complementary DNA (cDNA) synthesis was then performed using SuperScript IV One-Step RT-PCR system (Invitrogen; Thermo Fisher Scientific, Inc.). RT-qPCR was conducted using the SYBR-Green PCR Master Mix (Applied Biosystems; Thermo Fisher Scientific, Inc.) on ABI 7500 Real-time PCR system (Bio-Rad Laboratories, Inc.). The primer sequences used were listed as follows: ALOX5 forward, 5'-CCTCAGCCTCATTGGCTCTG-3' and reverse, 5'-TAGGAGTCCACCGCGCC-3'; GAPDH forward, 5'-CAGGAGAGTGTTTCCTCGTCC-3' and reverse, 5'-TTT GCCGTGAGTGGAGTCAT-3'. The mRNA expression was normalized to GAPDH and quantified using the comparative quantification method ($2^{-\Delta\Delta Cq}$) (25).

Western blotting. The cells were harvested using RIPA lysis buffer (Beyotime Institute of Biotechnology) to extract total protein. A bicinchoninic acid (BCA) kit (Sigma-Aldrich; Merck KGaA) was applied to measure the protein concentration according to the manufacturer's instructions. The same amount of protein (30 μg/lane) was electrophoresed on polyacrylamide gels and transferred to polyvinylidene

fluoride (PVDF) membranes (Millipore; Merck KGaA). After blocking with 5% skimmed milk for 2 h at room temperature, the membranes were incubated with primary antibodies against ALOX5 (1:1,000; cat. no. orb536948), Bcl-2 (1:1,000; cat. no. orb10173), Bax (1:2,000; cat. no. orb31066), and cleaved caspase-3 (1:1,000, cat. no. orb126608; all Biorbyt Ltd.), phosphorylated NF-κB inhibitor α (p-IκBα) (1:1,000; product no. 2859), IκBα (1:1,000; product no. 4812), p-p65 (1:1,000; product no. 3033), p65 (1:1,000; product no. 8242; all from Cell Signaling Technology, Inc.), collagen type IV (COL4; 1:1,000; cat. no. SAB4200500; Sigma-Aldrich; Merck KGaA), fibronectin (FN; 1:1,000; cat. no. 15613-1-AP; ProteinTech, Inc.), transforming growth factor (TGF)-β1 (1:1,000; cat. no. 21898-1-AP; ProteinTech, Inc.), and GAPDH (1:1,000; product no. 2118; Cell Signaling Technology, Inc.) at 4˚C overnight. The following day, the membranes were incubated with the horseradish peroxidase-conjugated goat anti-rabbit IgG secondary antibody (1:2,000; product code ab6721; Abcam) for 1 h at room temperature. The protein bands were visualized by enhanced chemiluminescence system (ECL; Thermo Fisher Scientific., Inc.) and quantified using ImageJ software version 1.46 (National Institutes of Health). Since GAPDH expression was not changed in HG-induced SV40 MES-13 cells in previous studies (22,24), GAPDH was used as the internal control.

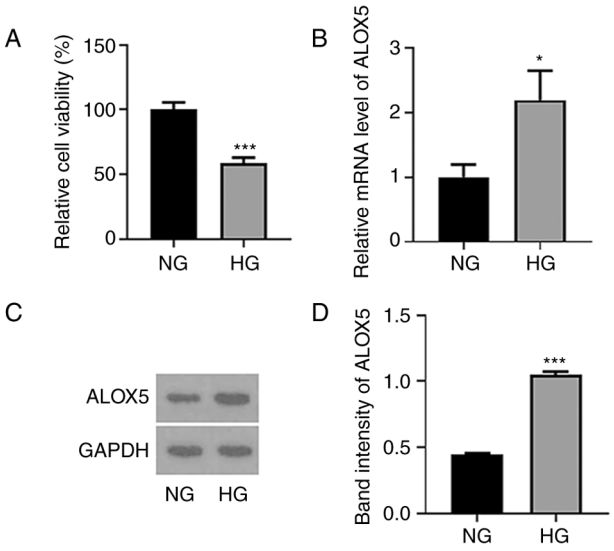

Figure 1. ALOX5 is upregulated in HG-induced SV40 MES-13 cells. (A) SV40 MES-13 cells were treated with HG (30 mM glucose) or NG (5.6 mM glucose) for 24 h, and the cell viability was detected using Cell Counting Kit-8 assay. (B) The mRNA level of ALOX5 was detected using reverse transcription-quantitative PCR. (C and D) The protein expression of ALOX5 was assessed using western blotting. *P<0.05 and ***P<0.001. ALOX5, 5-lipoxygenase; HG, high glucose; NG, normal glucose.

Statistical analysis. All data were analyzed using GraphPad Prism version 6 (GraphPad Software, Inc.) and presented as the mean ± standard deviation (SD) from at least three independent experiments. Comparisons between different groups were carried out using Student's unpaired t-test or one-way AVOVA followed by Tukey's post hoc test. P<0.05 was considered to indicate a statistically significant difference.

Results

ALOX5 is upregulated in HG-induced SV40 MES-13 cells. Firstly, SV40 MES-13 cells were treated with HG (30 mM glucose) for 24 h to simulate DN *in vitro*, and cells treated with NG (5.6 mM glucose) were regarded as the control. As revealed in Fig. 1A, the cell viability was significantly reduced following HG treatment. In addition, both the mRNA level and protein expression of ALOX5 were significantly upregulated upon HG treatment (Fig. 1B-D), suggesting that HG induced a high level of ALOX5 in SV40 MES-13 cells.

Silencing of ALOX5 promotes cell proliferation in HG-induced SV40 MES-13 cells. To investigate the role of ALOX5 in DN, SV40 MES-13 cells were transfected with si-ALOX5-1 or si-ALOX5-2 to silence ALOX5. As revealed in Fig. 2A and B, compared with si-control, both si-ALOX5-1 and si-ALOX5-2 significantly reduced the mRNA level and protein expression of ALOX5. Since the si-ALOX5-1 group was more efficient than the si-ALOX5-2 group in silencing ALOX5, it was used for subsequent experiments. A series of cellular experiments was then performed. As revealed in Fig. 2C, it was observed that at both 24 and 48 h post HG stimulation, the decreased cell viability under HG stimulation was significantly improved by ALOX5 silencing. Generally, the induction time is dependent on the induction efficacy and the research goal. In this study, upon 24 h of an induction of HG, a reduced cell viability was not only obtained, compared with NG, but a significantly upregulated expression level of ALOX5 was also found, confirming a high level of ALOX5 in HG-induced SV40 MES-13 cells, which was suitable for the following investigation on the specific role of ALOX5 upon HG stimulation. Thus, 24 h was the time-point used for investigation in this study. Subsequently, the expression levels of Ki67 and PCNA, two classical hallmarks of cell proliferation (26), were markedly decreased by HG treatment for 24 h, which were partly abolished by interference of ALOX5 (Fig. 2D and E). These results indicated that interference of ALOX5 improved cell proliferation ability of SV40 MES-13 cells under HG stimulation.

Silencing of ALOX5 promotes cell cycle progression and suppresses cell apoptosis in HG-induced SV40 MES-13 cells. Subsequently, a flow cytometric assay was conducted to analyze the effects of ALOX5 on cell cycle progression and cell apoptosis. As revealed in Fig. 3A, after treatment with HG, cells were arrested in the G1 phase, and the cell proportion in the S phase was reduced, reflecting that HG treatment blocked cell cycle progression. However, interference of ALOX5 reduced the cell proportion in the G1 phase and increased that in the S phase, indicating that interference of ALOX5 promoted the progression of the cell cycle. In addition, HG stimulation significantly increased the cell apoptosis rate of SV40 MES-13 cells, which was partly abolished by interference of ALOX5 (Fig. 3B). In addition, the reduced protein expression of Bcl-2 and the elevated protein expression of Bax and cleaved caspase-3 after HG induction were also partly hindered by silencing of ALOX5 (Fig. 3C). These results suggested that HG-induced blockage of cell cycle progression and a high rate of cell apoptosis could be partly attenuated by interference of ALOX5.

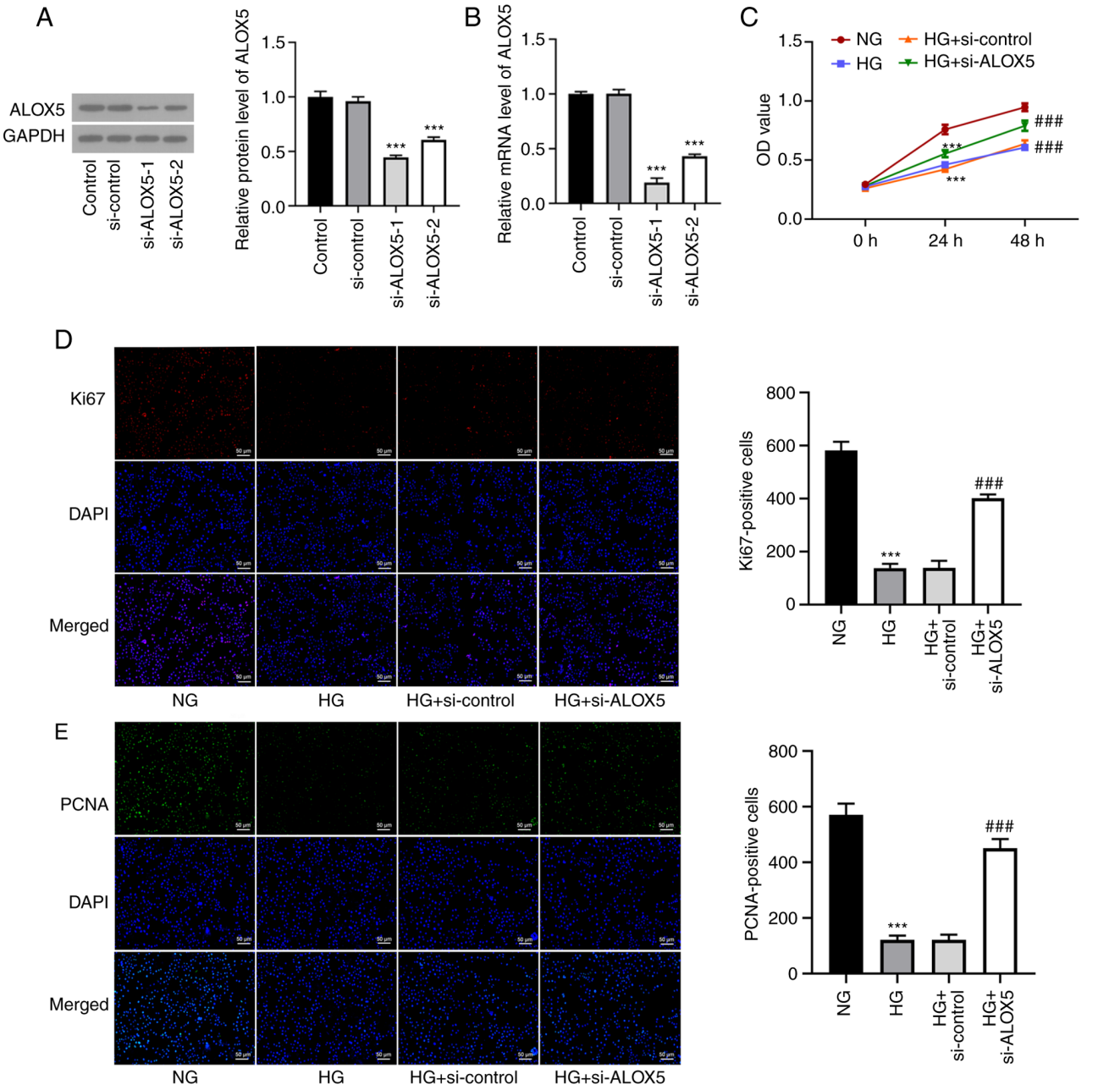

Figure 2. Silencing of ALOX5 promotes cell proliferation in HG-induced SV40 MES-13 cells. (A and B) SV40 MES-13 cells were transfected with si-ALOX5-1 or si-ALOX5-2 to silence ALOX5, and the protein expression and mRNA level of ALOX5 was assessed using (A) western blotting and (B) reverse transcription-quantitative PCR, respectively. ***P<0.001 vs. si-control. (C) The HG-induced SV40 MES-13 cells were transfected with si-ALOX5 or si-control, and the cell viability was detected using Cell Counting Kit-8 assay. (D) The expression level of Ki67 was detected using immunofluorescence. (E) The expression level of proliferating cell nuclear antigen was detected using immunofluorescence. ***P<0.001 vs. NG; ###P<0.001 vs. HG + si-control. ALOX5, 5-lipoxygenase; HG, high glucose; si-, siRNA; PCNA, proliferating cell nuclear antigen; NG, normal glucose.

Silencing of ALOX5 alleviates inflammatory response and fibrosis in HG-induced SV40 MES-13 cells. Next, a series of inflammatory cytokines and fibrosis-related proteins were assessed to detect the effects of ALOX5 on inflammation and fibrosis in a cell DN model *in vitro*. As shown in Fig. 4A-C, the upregulated levels of TNF-α, IL-6 and IL-8 upon HG stimulation were significantly suppressed when ALOX5 was silenced, indicating that silencing of ALOX5 markedly inhibited inflammatory response in HG-induced SV40 MES-13 cells. In addition, the upregulated protein expression levels of COL4, FN, and TGF-β1 upon HG stimulation were markedly inhibited by silencing of ALOX5 (Fig. 4D), suggesting that interference of ALOX5 attenuated HG-induced fibrosis.

Silencing of ALOX5 weakens NF-κB signaling pathway in HG-induced SV40 MES-13 cells. Finally, NF-κB, as an important inflammatory stimulus for DN (27,28), was also assessed in the present study. As revealed in Fig. 5, HG stimulation enhanced the expression levels of p-IκBα and p-p65, indicating that NF-κB signaling was activated upon HG stimulation, whereas silencing of ALOX5 reduced the expression levels of p-IκBα and p-p65. These results indicated that ALOX5 regulated NF-κB activation.

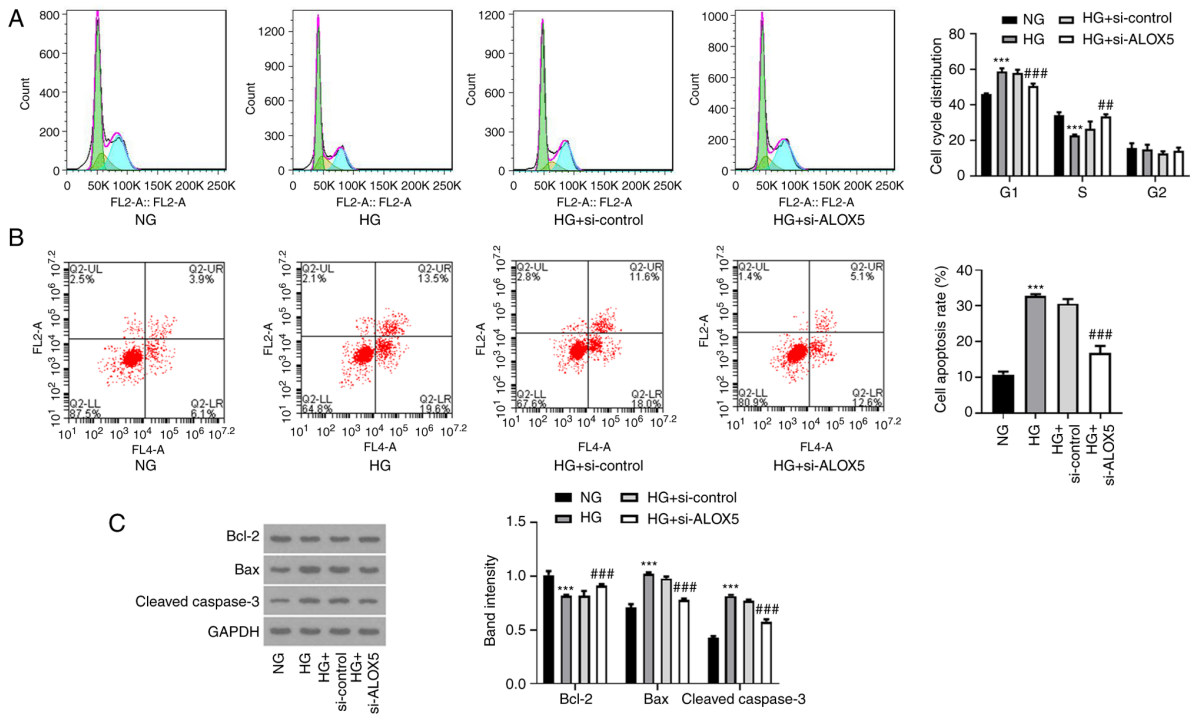

Figure 3. Silencing of ALOX5 promotes cell cycle progression and suppresses cell apoptosis in HG-induced SV40 MES-13 cells. (A) The HG-induced SV40 MES-13 cells were transfected with si-ALOX5 or si-control, and the cell cycle distribution of each group was assessed by flow cytometric analysis. The green region indicates the G1 phase; the yellow region indicates the S phase; the blue region indicates the G2 phase. (B) The cell apoptosis rate of each group was evaluated by flow cytometric analysis. (C) The expression of apoptosis-related proteins, including Bcl-2, Bax and cleaved caspase-3, were assessed using western blotting. ***P<0.001 vs. NG; $^{\#\#}$P<0.01 and $^{\#\#\#}$P<0.001 vs. HG + si-control. ALOX5, 5-lipoxygenase; HG, high glucose; si-, siRNA; NG, normal glucose.

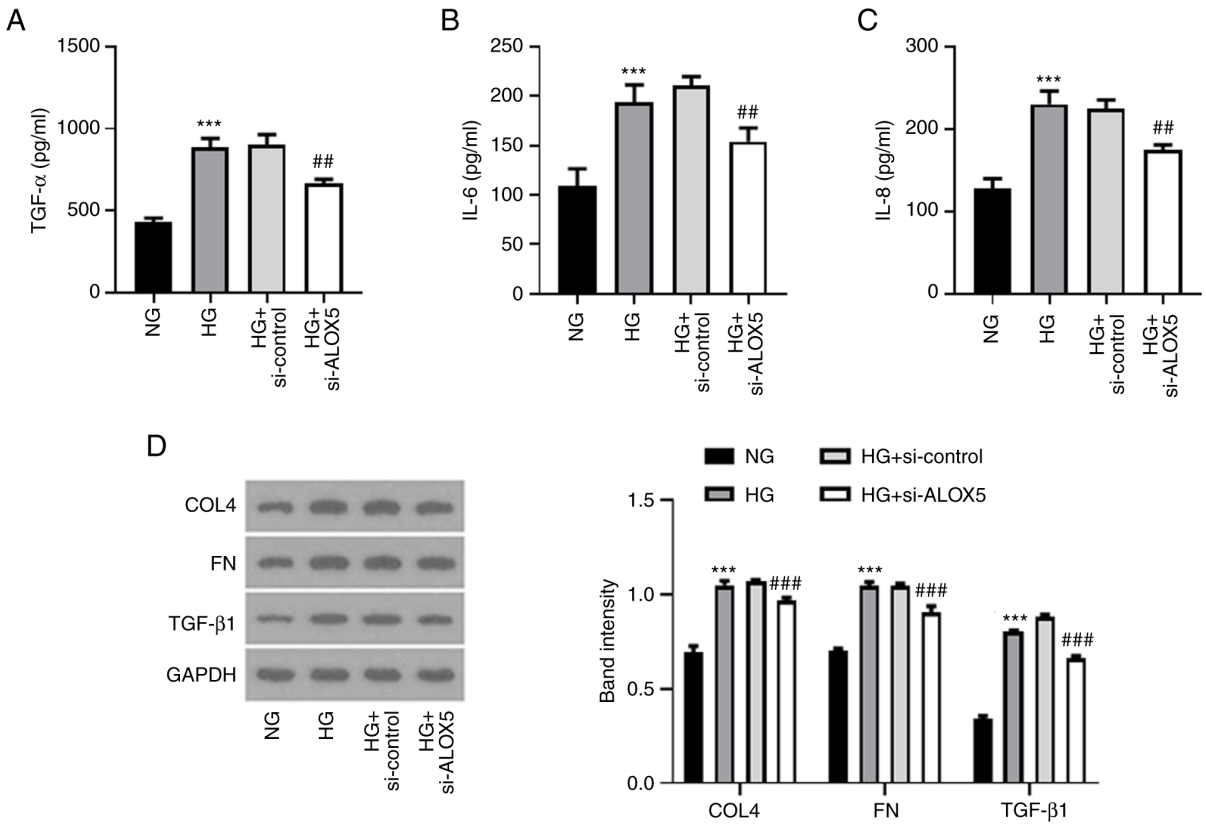

Figure 4. Silencing of ALOX5 alleviates inflammatory response and fibrosis in HG-induced SV40 MES-13 cells. (A-C) The HG-induced SV40 MES-13 cells were transfected with si-ALOX5 or si-control, and the inflammatory cytokines, including TNF-α, IL-6 and IL-8 were evaluated using their corresponding ELISA kits. (D) The expression level of fibrosis-related proteins was assessed using western blotting. ***P<0.001 vs. NG; $^{\#\#}$P<0.01 and $^{\#\#\#}$P<0.001 vs. HG + si-control. ALOX5, 5-lipoxygenase; HG, high glucose; si-, siRNA; ELISA, enzyme-linked immunosorbent; NG, normal glucose; COL4, collagen type IV; FN, fibronectin; TGF-β1, transforming growth factor β1.

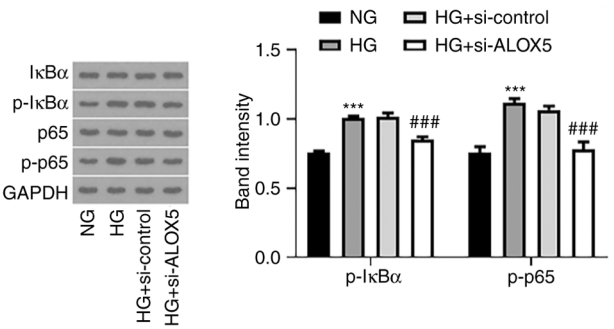

Figure 5. Silencing of ALOX5 weakens the NF-κB signaling pathway in HG-induced SV40 MES-13 cells. The HG-induced SV40 MES-13 cells were transfected with si-ALOX5 or si-control, and the protein expression of p-IκBα, IκBα, p-p65, and p65 was measured using western blotting. ***P<0.001 vs. NG; ###P<0.001 vs. HG + si-control. ALOX5, 5-lipoxygenase; HG, high glucose; si-, siRNA; p-, phosphorylated; IκBα, NF-κB inhibitor α; NG, normal glucose.

Discussion

DN is one of the most challenging kidney diseases. This disease leads to heavy financial and health-care burdens globally (29), therefore, it is evident that further understanding of the pathogenic mechanisms underlying DN is urgently required to prevent disease progression. Firstly, to better carry out our investigation, an *in vitro* cell model of DN was firstly constructed. HG-induced SV40 MES-13 has been widely recognized as an *in vitro* cell model of DN, and has been widely applied in numerous studies (21-24). In addition, mannitol is usually used as a negative control to eliminate the effects of osmotic pressure caused by HG; however, in a previous study mannitol did not produce any change in comparison with the control, indicating that osmotic pressure is not a variable factor between NG and HG (24), thus numerous studies only set NG and HG, without mannitol as a negative control, for the investigation in HG-induced kidney injury (21-23). Accordingly, the present study used NG and HG groups for the investigation. In the present study, it was observed that ALOX5 was aberrantly upregulated by HG stimulation in SV40 MES-13 cells. A series of cellular biological experiments revealed that silencing of ALOX5 could efficiently attenuate HG-induced renal cell injuries by mitigating cell apoptosis and cell growth restriction, antagonizing inflammatory response and fibrosis in SV40 MES-13 cells. Mechanistically, interference of ALOX5 inhibited NF-κB signaling, which may account for the regulatory function of ALOX5 in HG-induced SV40 MES-13 cells. These results suggested that ALOX5 may serve as a promising candidate for novel therapeutic strategies of DN treatment. Furthermore, silencing of ALOX5 exerted a protective effect against HG-induced injuries in SV40 MES-13 cells, raising the possibility that ALOX5 inhibitors or ALOX5-targeting drugs may be alternative strategies for the clinical treatment of DN.

DN is a multifactorial disease involving a variety of pathogenic molecular processes and histopathological structure. Fibrosis and inflammation are important pathologic characteristics of DN. The production of fibrotic and pro-inflammatory cytokines can directly damage the kidney structure and promote the deposition of extracellular matrix components (EMC), thereby contributing to the onset and progression of DN (30,31). In addition, apoptosis is a strictly controlled cell death process, which is involved in cell growth in multiple diseases. It was reported by Zheng *et al* that HG treatment promoted the apoptosis of mouse β-TC-tet cells, and that cell apoptosis was up to 30% (32). In addition, another study revealed that the apoptosis rate of RSC96 Schwann cells was increased to ~40% following HG treatment for 48 h (33). However, according to different handling factors such as experiment personnel, there may exist some differences in the actual data between different studies. In the present study, promotion of apoptosis (~30%) was demonstrated following HG treatment for 24 h in SV40 MES-13 cells, indicating that HG caused severe injury in renal cells. The accumulating evidence confirms that renal cell apoptosis is also a classical hallmark of DN, whereby apoptotic cells may be partly attributed to renal inflammation (34,35). Qi *et al* determined that NORAD could aggravate the progression of DN by promoting the proliferative ability and inhibiting the apoptosis of glomerular mesangial cells (21). Ma *et al* reported that downregulation of lncRNA NEAT1 inhibited cell proliferation, fibrosis, and inflammation but promoted cell apoptosis in a DN cellular model, shedding light on the application of lncRNA NEAT1 downregulation in the treatment of DN (36). It was also demonstrated by Liu *et al* that praliciguat inhibited the progression of DN partly by suppressing inflammation and apoptosis (37). Consistently, in the present study, it was determined that silencing of ALOX5 not only exerted anti-inflammatory and anti-fibrotic effects, but also exerted anti-apoptotic effects, accompanied with the promotive effects on cell viability, Ki67-positive and PCNA-positive cells, and cell cycle progression. These results provided ample evidence that silencing of ALOX5 could retain anti-fibrosis, anti-inflammation and anti-apoptosis, thereby suppressing the progression of DN, revealing the potential application of ALOX5 interference for the treatment of DN.

Furthermore, NF-κB signaling has been demonstrated to be a key inflammatory pathway in the pathogenesis of DN inflammation and fibrosis in both clinical and animal studies (28,38). Under normal conditions, NF-κB binds to anchor protein IκBα, forming an inactive complex in the cytoplasm, which suppresses the activation of NF-κB signaling (39). In a diabetic state, IκBα can be phosphorylated in its proteasomal degradation by the IKK complex, leading to the activation and phosphorylation of NF-κB subunit p65, which is then translocated towards the nucleus and triggers the overproduction of pro-inflammatory cytokines, including TNF-α and IL-6. Particularly, the hyperphosphorylation of IκBα and p65 have been observed in DN *in vivo* or *in vitro*, confirming that DN was dependent on NF-κB activation, and limiting the activation of NF-κB has been widely demonstrated to protect the rats against DN (27,40-42). Consistently, the present study also demonstrated the hyperphosphorylation of IκBα and p65, as well as a severe inflammatory response, in HG-induced SV40 MES-13 cells. In addition, it has been reported that ALOX5 and its metabolite LTB4 are capable of activating NF-κB in cancer cells, indicating a close association between ALOX5 and NF-κB and a potential regulatory effect of ALOX5 on NF-κB signaling (43,44). In the present study, it was further demonstrated that silencing of ALOX5 downregulated p-p65 and p-IκBα in HG-induced SV40 MES-13 cells, revealing that interference of ALOX5 could regulate the functional NF-κB subunit to block HG-induced activation of NF-κB signaling in a DN cell model *in vitro*.

Although the role of ALOX5 in HG-induced SV40 MES-13 cells was investigated in the present study, thus far, these findings have not been verified *in vivo* or clinically. In addition, whether glomerular mesangial cells express ALOX5 under normal or disease conditions *in vivo* should be verified in future studies. Furthermore, despite the fact that silencing of ALOX5 was determined to suppress NF-κB signaling in HG-induced SV40 MES-13 cells, whether the effect of ALOX5 is NF-κB-dependent remains to be investigated. Moreover, all of the findings concerning the cellular biological activities in the present study were based on transfection with si-ALOX5-1, therefore, a second siRNA may be beneficial to verify the absence of off-target effects. In addition, the involvement of other signaling pathways underlying the regulatory role of ALOX5 in HG-induced renal injury cannot be excluded. Further studies are required to reveal the functions and precise mechanisms of ALOX5 in DN *in vivo* and *in vitro*.

In conclusion, it was demonstrated that ALOX5 was aberrantly upregulated in HG-induced renal cell injury, and silencing of ALOX5 ameliorated DN *in vitro* by attenuating the inflammatory response, fibrosis and cell apoptosis. Mechanistic analysis revealed the importance of NF-κB signaling underlying the regulation of ALOX5 in DN. The present study contributed to an improved understanding of the mechanism underlying ALOX5 involved in DN. ALOX5 may be considered as an attractive therapeutic target to prevent the development of DN.

Acknowledgements

Not applicable.

Funding

No funding was received.

Availability of data and materials

All data generated and/or analyzed during the present study are included in this published article.

Authors' contributions

XC designed the study. XC, HX, YL, QO and SD conducted the experiments and analyzed the data. HX drafted the manuscript and XC revised the manuscript. All authors read and approved the final manuscript.. XC and HX confirm the authenticity of all the raw data and are agreed to be accountable for all aspects of the work.

Ethics approval and consent to participate

Not applicable.

Patient consent for publication

Not applicable.

Competing interests

The authors declare that they have no competing interests.

References

1. Sagoo MK and Gnudi L: Diabetic nephropathy: An overview. Methods Mol Biol 2067: 3-7, 2020.
2. Gheith O, Farouk N, Nampoory N, Halim MA and Al-Otaibi T. Diabetic kidney disease: World wide difference of prevalence and risk factors. J Nephropharmacol 5: 49-56, 2016.
3. Narres M, Claessen H, Droste S, Kvitkina T, Koch M, Kuss O and Icks A: The incidence of end-stage renal disease in the diabetic (compared to the non-diabetic) population: A systematic review. PLoS One 11: e0147329, 2016.
4. Si X, Li P, Zhang Y, Zhang Y, Lv W and Qi D. Renoprotective effects of olmesartan medoxomil on diabetic nephropathy in streptozotocin-induced diabetes in rats. Biomed Rep 2: 24-28, 2014.
5. Shi Y and Hu FB: The global implications of diabetes and cancer. Lancet 383: 1947-1948, 2014.
6. Weir MA and Herzog CA: Beta blockers in patients with end-stage renal disease-evidence-based recommendations. Semin Dial 31: 219-225, 2018.
7. Dobrian AD, Lieb DC, Cole BK, Taylor-Fishwick DA, Chakrabarti SK and Nadler JL: Functional and pathological roles of the 12- and 15-lipoxygenases. Prog Lipid Res 50: 115-131, 2011.
8. Chen F, Ghosh A, Lin J, Zhang C, Pan Y, Thakur A, Singh K, Hong H and Tang S: 5-lipoxygenase pathway and its downstream cysteinyl leukotrienes as potential therapeutic targets for Alzheimer's disease. Brain Behav Immun 88: 844-855, 2020.
9. Wang Y, Skibbe JR, Hu C, Dong L, Ferchen K, Su R, Li C, Huang H, Weng H, Huang H, *et al*: ALOX5 exhibits anti-tumor and drug-sensitizing effects in MLL-rearranged leukemia. Sci Rep 7: 1853, 2017.
10. Lisovyy OO, Dosenko VE, Nagibin VS, Tumanovska LV, Korol MO, Surova OV and Moibenko OO: Cardioprotective effect of 5-lipoxygenase gene (ALOX5) silencing in ischemia-reperfusion. Acta Biochim Pol 56: 687-694, 2009.
11. Wu Y, Sun H, Song F, Huang C and Wang J: Deletion of Alox5 gene decreases osteogenic differentiation but increases adipogenic differentiation of mouse induced pluripotent stem cells. Cell Tissue Res 358: 135-147, 2014.
12. Zhu L, Yang F, Wang L, Dong L, Huang Z, Wang G, Chen G and Li Q: Identification the ferroptosis-related gene signature in patients with esophageal adenocarcinoma. Cancer Cell Int 21: 124, 2021.
13. Tang J, Zhang C, Lin J, Duan P, Long J and Zhu H: ALOX5-5-HETE promotes gastric cancer growth and alleviates chemotherapy toxicity via MEK/ERK activation. Cancer Med 10: 5246-5255, 2021.
14. Heemskerk MM, Giera M, Bouazzaoui FE, Lips MA, Pijl H, van Dijk KW and van Harmelen V: Increased PUFA content and 5-Lipoxygenase pathway expression are associated with subcutaneous adipose tissue inflammation in obese women with type 2 diabetes. Nutrients 7: 7676-7690, 2015.
15. ul Ain Q, Greig NH, Nawaz MS, Rashid S and Kamal MA: Exploring N(1)-p-fluorobenzyl-cymserine as an inhibitor of 5-lipoxygenase as a candidate for type 2 diabetes and neurodegenerative disorder treatment. CNS Neurol Disord Drug Targets 13: 197-202, 2014.
16. Ramalho T, Filgueiras L, Silva-Jr IA, Pessoa AFM and Jancar S: Impaired wound healing in type 1 diabetes is dependent on 5-lipoxygenase products. Sci Rep 8: 14164, 2018.
17. Schwartzman ML, Iserovich P, Gotlinger K, Bellner L, Dunn MW, Sartore M, Grazia Pertile M, Leonardi A, Sathe S, Beaton A, *et al*: Profile of lipid and protein autacoids in diabetic vitreous correlates with the progression of diabetic retinopathy. Diabetes 59: 1780-1788, 2010.
18. Gubitosi-Klug RA, Talahalli R, Du Y, Nadler JL and Kern TS: 5-Lipoxygenase, but not 12/15-lipoxygenase, contributes to degeneration of retinal capillaries in a mouse model of diabetic retinopathy. Diabetes 57: 1387-1393, 2008.
19. Landgraf SS, Silva LS, Peruchetti DB, Sirtoli GM, Moraes-Santos F, Portella VG, Silva-Filho JL, Pinheiro CS, Abreu TP, Takiya CM, *et al*: 5-Lypoxygenase products are involved in renal tubulointerstitial injury induced by albumin overload in proximal tubules in mice. PLoS One 9: e107549, 2014.
20. Reinhold SW, Vitzthum H, Filbeck T, Wolf K, Lattas C, Riegger GA, Kurtz A and Krämer BK: Gene expression of 5-, 12-, and 15-lipoxygenases and leukotriene receptors along the rat nephron. Am J Physiol Renal Physiol 290: F864-F872, 2006.

21. Qi H, Yao L and Liu Q: NORAD affects the progression of diabetic nephropathy through targeting miR-520h to upregulate TLR4. Biochem Biophys Res Commun 521: 190-195, 2020.
22. Du Y, Yang YT, Tang G, Jia JS, Zhu N and Yuan WJ: Butyrate alleviates diabetic kidney disease by mediating the miR-7a-5p/P311/TGF-beta1 pathway. FASEB J 34: 10462-10475, 2020.
23. Yang X, Luo W, Li L, Hu X, Xu M, Wang Y, Feng J, Qian J, Guan X, Zhao Y and Liang G: CDK9 inhibition improves diabetic nephropathy by reducing inflammation in the kidneys. Toxicol Appl Pharmacol 416: 115465, 2021.
24. Xu J, Xiang P, Liu L, Sun J and Ye S: Metformin inhibits extracellular matrix accumulation, inflammation and proliferation of mesangial cells in diabetic nephropathy by regulating H19/miR-143-3p/TGF-β1 axis. J Pharm Pharmacol 72: 1101-1109, 2020.
25. Livak KJ and Schmittgen TD: Analysis of relative gene expression data using real-time quantitative PCR and the 2(-Delta Delta C(T)) method. Methods 25: 402-408, 2001.
26. Jurikova M, Danihel L, Polak S and Varga I: Ki67, PCNA, and MCM proteins: Markers of proliferation in the diagnosis of breast cancer. Acta Histochem 118: 544-552, 2016.
27. Liu T, Zhang L, Joo D and Sun SC: NF-κB signaling in inflammation. Signal Transduct Target Ther 2: 17023, 2017.
28. Donate-Correa J, Martín-Núñez E, Muros-de-Fuentes M, Mora-Fernández C and Navarro-González JF: Inflammatory cytokines in diabetic nephropathy. J Diabetes Res 2015: 948417, 2015.
29. Samsu N: Diabetic nephropathy: Challenges in pathogenesis, diagnosis, and treatment. Biomed Res Int 2021: 1497449, 2021.
30. Moreno JA, Gomez-Guerrero C, Mas S, Sanz AB, Lorenzo O, Ruiz-Ortega M, Opazo L, Mezzano S and Egido J: Targeting inflammation in diabetic nephropathy: A tale of hope. Expert Opin Investig Drugs 27: 917-930, 2018.
31. Chow FY, Nikolic-Paterson DJ, Ozols E, Atkins RC and Tesch GH: Intercellular adhesion molecule-1 deficiency is protective against nephropathy in type 2 diabetic db/db mice. J Am Soc Nephrol 16: 1711-1722, 2005.
32. Zheng H, Li X, Yang X, Yan F, Wang C and Liu J: miR-217/Mafb axis involve in high glucose-induced β-TC-tet cell damage via regulating NF-κB signaling pathway. Biochem Genet 58: 901-913, 2020.
33. Dong J, Li H, Bai Y and Wu C: Muscone ameliorates diabetic peripheral neuropathy through activating AKT/mTOR signalling pathway. J Pharm Pharmacol 71: 1706-1713, 2019.
34. Rane MJ, Song Y, Jin S, Barati MT, Wu R, Kausar H, Tan Y, Wang Y, Zhou G, Klein JB, *et al*: Interplay between Akt and p38 MAPK pathways in the regulation of renal tubular cell apoptosis associated with diabetic nephropathy. Am J Physiol Renal Physiol 298: F49-F61, 2010.
35. Yu Q, Zhang M, Qian L, Wen D and Wu G: Luteolin attenuates high glucose-induced podocyte injury via suppressing NLRP3 inflammasome pathway. Life Sci 225: 1-7, 2019.
36. Ma J, Zhao N, Du L and Wang Y: Downregulation of lncRNA NEAT1 inhibits mouse mesangial cell proliferation, fibrosis, and inflammation but promotes apoptosis in diabetic nephropathy. Int J Clin Exp Pathol 12: 1174-1183, 2019.
37. Liu G, Shea CM, Jones JE, Price GM, Warren W, Lonie E, Yan S, Currie MG, Profy AT, Masferrer JL and Zimmer DP: Praliciguat inhibits progression of diabetic nephropathy in ZSF1 rats and suppresses inflammation and apoptosis in human renal proximal tubular cells. Am J Physiol Renal Physiol 319: F697-F711, 2020.
38. Oguiza A, Recio C, Lazaro I, Mallavia B, Blanco J, Egido J and Gomez-Guerrero C: Peptide-based inhibition of IκB kinase/nuclear factor-κB pathway protects against diabetes-associated nephropathy and atherosclerosis in a mouse model of type 1 diabetes. Diabetologia 58: 1656-1667, 2015.
39. Schröfelbauer B, Polley S, Behar M, Ghosh G and Hoffmann A: NEMO ensures signaling specificity of the pleiotropic IKKβ by directing its kinase activity toward IκBα. Mol Cell 47: 111-121, 2012.
40. Manna K, Mishra S, Saha M, Mahapatra S, Saha C, Yenge G, Gaikwad N, Pal R, Oulkar D, Banerjee K and Das Saha K: Amelioration of diabetic nephropathy using pomegranate peel extract-stabilized gold nanoparticles: Assessment of NF-κB and Nrf2 signaling system. Int J Nanomedicine 14: 1753-1777, 2019.
41. Zhang Y, Ren S, Ji Y and Liang Y: Pterostilbene ameliorates nephropathy injury in streptozotocin-induced diabetic rats. Pharmacology 104: 71-80, 2019.
42. Kolati SR, Kasala ER, Bodduluru LN, Mahareddy JR, Uppulapu SK, Gogoi R, Barua CC and Lahkar M: BAY 11-7082 ameliorates diabetic nephropathy by attenuating hyperglycemia-mediated oxidative stress and renal inflammation via NF-κB pathway. Environ Toxicol Pharmacol 39: 690-699, 2015.
43. Zhao Y, Wang W, Wang Q, Zhang X and Ye L: Lipid metabolism enzyme 5-LOX and its metabolite LTB4 are capable of activating transcription factor NF-κB in hepatoma cells. Biochem Biophys Res Commun 418: 647-651, 2012.
44. Cheng JH, Zhang WJ, Zhu JF, Cui D, Song KD, Qiang P, Mei CZ, Nie ZC, Ding BS, Han Z, *et al*: CaMKIIγ regulates the viability and self-renewal of acute myeloid leukaemia stem-like cells by the Alox5/NF-κB pathway. Int J Lab Hematol 43: 699-706, 2021.